Molecular analysis of enthesopathy in a mouse model of hypophosphatemic rickets

Eva S. Liu,[1,2,3] Janaina S. Martins,[2,3] Wanlin Zhang,[2] and Marie B. Demay[2,3]

[1]Division of Endocrinology, Diabetes, and Hypertension
Brigham and Women's Hospital, Boston, Massachusetts 02115

[2]Endocrine Unit
Massachusetts General Hospital, Boston, Massachusetts 02114

[3]Harvard Medical School
Boston, Massachusetts 02115

Correspondence should be addressed to:
Marie Demay
Endocrine Unit, Massachusetts General Hospital,
50 Blossom Street, Thier 11,
Boston, MA 02114
Fax: 617-726-7543
Tel: 617-726-3273,
Email: demay@helix.mgh.harvard.edu

All authors have declared that no conflict of interest exists.

Key words: enthesis, tendon-bone attachment, XLH, BMP, IHH, 1,25 dihydroxyvitamin D, phosphate, FGF23

Summary Statement:

The BMP and IHH signaling pathways play a role in normal post-natal enthesis maturation. Misregulation of these pathways contributes to the development of enthesopathy in X-linked hypophosphatemia.

Abstract:

The bone tendon attachment site known as the enthesis is comprised of a transitional zone between bone and tendon and plays an important role in enabling movement at this site. X-linked hypophosphatemia (XLH) is characterized by impaired activation of vitamin D, elevated serum FGF23 levels and low serum phosphate levels, which impair bone mineralization. Paradoxically, an important complication of XLH is mineralization of the enthesis (enthesopathy). Studies were undertaken to identify the cellular and molecular pathways important for normal post-natal enthesis maturation and to examine their role during the development of enthesopathy in mice with XLH (Hyp). The Achilles tendon entheses of Hyp mice demonstrate an expansion of hypertrophic-appearing chondrogenic cells by P14. Post-natally cells in WT and Hyp entheses similarly descend from Scleraxis and Sox9 expressing progenitors, however, Hyp entheses exhibit an expansion of Sox9-expressing cells and enhanced BMP and IHH signaling. These results support a role for enhanced BMP and IHH signaling in the development of enthesopathy in XLH.

Introduction:

The enthesis is a specialized tissue that forms at the site of attachment of tendon to bone, optimizing the transfer of mechanical stress and force from muscle to bone, allowing for limb and body movement (Zelzer et al., 2014). The fibrocartilaginous transitional zone between bone and tendon consists of 4 zones, including the bony eminence, mineralized fibrocartilage, unmineralized fibrocartilage, and tendon (Zelzer et al., 2014). This region is characterized by a gradual increase in mineral content and a characteristic distribution of collagens and proteoglycans (Genin et al., 2009; Schwartz et al., 2012).

The bHLH transcription factor Scleraxis (Scx), a specific marker for tendon and ligament progenitors, is required for formation of force-transmitting and intermuscular tendons as well as a functional enthesis (Schweitzer et al., 2001; Murchison et al., 2007; Killian and Thomopoulos, 2016). During embryonic development, the bony eminence onto which tendons insert expresses both Scx and Sox9, the latter of which is a BMP target gene that marks chondroprogenitor cells during endochondral bone formation (Bi et al., 1999); however, the cells closest to bone are more likely to arise from Sox9 progenitors (Akiyama et al., 2005; Sugimoto et al., 2013). The BMP pathway has been implicated in inducing chondrocyte cell fate during development of the deltoid tuberosity into which tendons insert (Minina et al., 2001; Kumar et al., 2012). Consistent with this, factors that regulate chondrocyte differentiation, including Indian Hedgehog (IHH) and its receptor Patched (PTCH), are expressed in the enthesis (Chen et al., 2006; Thomopoulos et al., 2010; Liu et al., 2012). Of note, IHH which is secreted by prehypertrophic and early hypertrophic chondrocytes (St-Jacques et al., 1999; Kronenberg, 2003), has been implicated in the pathogenesis of pathologic ligament ossification (Sugita et al., 2013).

X-linked hypophosphatemia (XLH) is the most common form of hypophosphatemic rickets, with an incidence of 1:20,000 in the general population (Carpenter et al., 2011). It is characterized by a mutation in PHEX, leading to elevated serum FGF23 levels, hypophosphatemia, and suppression of the vitamin D 1-alpha-hydroxyase (Holm et al., 1997; Jonsson et al., 2003; Liu et al., 2006). This results in rickets and impaired mineralization of bone. A significant complication of XLH in adults is the paradoxical mineralization of the tendon-bone attachment site (enthesopathy), which results in pain, impaired movement, and decreased quality of life (Liang et al., 2009). The molecular and cellular basis of the enthesopathy in XLH is poorly understood. Therefore, studies in the murine model of XLH (Hyp) were undertaken to address the origin of aberrant cells that give rise to the enthesopathy, as well as to identify roles for BMP and IHH signaling pathways in the pathogenesis of enthesopathy. Since previous studies have focused on normal enthesis development during embryogenesis, these studies also provide insight into the molecular and cellular pathways involved in normal post-natal enthesis maturation.

Materials and Methods:

Study Design: The purpose of these studies is to characterize the phenotype of the enthesopathy observed in Hyp mice with XLH. Lineage tracing studies were performed to determine the origin of the abnormal cells observed in Hyp entheses. Immunohistochemical, histological, and gene expression analyses were performed to identify markers and signaling pathways that are aberrantly expressed in the Hyp entheses. To examine if improving phosphate and 1,25D homeostasis or blocking FGF23 action prevents the development of Hyp enthesopathy, Hyp mice were treated with 1,25D or an anti-FGF23 blocking antibody (FGF23Ab).

Animal Studies: Animal studies were approved by the institutional animal care committee. All mice were on a C57BL/6J background, maintained in a virus and parasite free barrier facility and exposed to a 12 hour light/dark cycle. Mice were weaned day 18 onto house chow (1% calcium, 0.6% phosphate) and housed in up to 5 mice per cage.

Male and female wild type (WT), Hyp, Scx-GFP (Pryce et al., 2007), Sox9-CreERT2 (Soeda et al., 2010), Scx-Cre (Blitz et al., 2009), Scx-CreERT2 (Howell et al., 2017), and Rosa26-loxP-stop-loxP-TdTomato ($R26R^{Tom}$ mice, JAX 7914) mice were studied. Scx-GFP mice were crossed to Hyp mice to examine Scx expression in entheses of WT and Hyp mice. The Scx-Cre, Sox9-CreERT, and Scx-CreERT2 mice were crossed to the $R26R^{Tom}$ mice, and the resultant Scx-Cre; $R26R^{Tom}$, Sox9-CreERT2; $R26R^{Tom}$, and Scx-CreERT2; $R26R^{Tom}$ mice were mated to the Hyp mice. For lineage tracing experiments using the Sox9-CreERT2 and Scx-CreERT2 mice, intraperitoneal injections of tamoxifen (0.1 mg/g, Sigma) dissolved in sunflower oil were performed on P2. Tamoxifen-injected Sox9-CreERT2 mice were sacrificed on P5, P14, and P30 and tamoxifen-injected Scx-CreERT2 mice were sacrificed on P14.

Male and female Hyp mice were injected daily with 1,25D (175 pg/g/day, Akorn, Inc.) or 3 times per week with FGF23Ab (35 mcg/g, Amgen) starting on P2. Wild type and Hyp control littermates of both sexes received vehicle or isotype matched antibody (35 mcg/g).

Histology: The Achilles tendon entheses were dissected from mice, fixed in 10% formalin/PBS, decalcified in 20% EDTA/PBS (pH 8.0), and processed for paraffin sections. For frozen sections, decalcified entheses were embedded in OCT and cryosectioned at 5 μm. Immunofluroescent images were captured with an epifluoresence microscope (Nikon Eclipse E800) with prefigured triple band filter settings for DAPI/FITC/TRITC.

To evaluate alkaline phosphatase, P75 entheses were fixed in 70% alcohol and processed for resin embedded sections. P5, P14, and P30 entheses were fixed in 10% formalin and processed for frozen sections. Deplasticized or frozen sections were immersed in Tris Buffer pH 9.4 for 1 hour and then incubated in alkaline phosphate staining solution (Tris Buffer pH 9.4, Fast Blue solution, Napthol ASBI Phosphate solution, and magnesium chloride) at room temperature.

Immunohistochemistry: Paraffin sections were rehydrated and blocked with TNB (0.1M Tris-HCL pH 7.5, 0.15M NaCl, 0.5% blocking reagent (Perkin Elmer)). For Sox9 immunohistochemistry, antigen retrieval was performed by incubating with trypsin (Sigma) at 37°C, while for p-Smad1/5/9 and Runx2 immunohistochemistry, sections were incubated with Proteinase K at 37°C. After incubation with primary antibody (anti-Sox9 antibody (1:2000, Millipore, AB5535), anti-p-Smad1/5/9 antibody (1:100, Cell Signaling, 13820), or anti-Runx2 antibody (1:800, Cell Signaling, 12556), signal detection was performed using biotinylated goat-anti rabbit secondary antibody (Vector) followed by amplification with the TSA^{TM} Kit (Perkin Elmer). For Patched immunohistochemistry, paraffin sections were subjected to antigen retrieval with trypsin and blocked with 10% heat inactivated fetal bovine serum (hi-FBS) in PBS. Following incubation with anti-Patched antibody (1:300, AbCam, ab53715), signal was detected using a goat anti-rabbit HRP antibody (Sigma). For proliferating cell nuclear antigen (PCNA) immunohistochemistry, paraffin sections were blocked with 10% hi-FBS in PBS, then incubated with anti-PCNA antibody (1:100, Thermo-Fisher Scientific, 13-3900). Signal was detected using a biotinylated goat anti-mouse secondary antibody (Vector) followed by incubation with streptavidin conjugated with horseradish perioxidase (Perkin Elmer).

For Sox9 immunohistochemistry on frozen sections, sections were equilibrated to room temperature, blocked with 10% hi-FBS/PBS, and incubated with anti-Sox9 antibody (1:250). Fluorescent signal was detected using Alexa-Fluor -546 conjugated donkey anti-rabbit antibody (Invitrogen).

The number of alkaline phosphatase positive, percent Safranin O or Scx-Tomato positive, and percent immunoreactive cells in the entheses were quantitated. The enthesis region was defined on one side by the distal border of the calcaneal secondary ossification center and on the other end by the point where the anterior part of the tendon emerges from the articular surface.

The ratio of the number of immunoreactive, Safranin O positive, or Scx-Tomato positive cells to the total number of cells in the defined enthesis region was calculated.

Enthesis RNA Analysis: The site at which the P14 WT and Hyp Achilles tendon insert into the calcaneus was identified under a dissection microscope (Nikon) at 5x magnification and isolated using a microsurgical knife by slicing through the proximal end of the tendon and the region adjacent to the distal portion of the calcaneus. The enthesis tissue was homogenized in Trizol (Thermo Scientific Fisher). Total RNA was precipitated using 100% ethanol and purified using the PureLink^{TM} RNA mini kit (Thermo Fisher Scientific).

In vitro chondrocyte studies. Primary chondrocytes were isolated from P2 wild type murine ribs and cultured as previously described (Sabbagh et al., 2005). Chondrocytes cultured for 48 hours were serum restricted (0.5% FBS) and treated with 10^{-8} M 1,25D 18 hours prior to exposure to recombinant human BMP2 (rhBMP2) (150 ng/mL) for 4 hours. Chondrocytes were harvested after 72 hours in culture for isolation of RNA using a PureLink^{TM} RNA mini kit (Thermo Fisher Scientific).

Gene expression analyses. RNA was reverse transcribed with PrimeScript^{TM} (Takara-Clontech). Quantitative real time-PCR was performed using the QuantiTect SYBR Green RT-PCR kit (Qiagen) on an Opticon DNA engine (MJ Research). Gene expression was normalized to that of a control gene for each sample, using the methods of Livak and Schmittgen.(Miedlich et al., 2010)

Serum parameters. Serum calcium and phosphate were measured using a HESKA DRI CHEM 7000 veterinary analyzer (Liu et al., 2016).

Statistical Analysis. All data shown are reported as mean ± standard error of the mean (SEM). Student's two-tailed T-test was used to determine significance between WT and Hyp groups. One-way ANOVA followed by Fisher's least significant difference (LSD) test was used to analyze significance between all control and 1,25D or FGF23Ab treated groups. Significance was defined as a $P< 0.05$. GraphPad Prism software was used for all data analysis.

Results:

WT and Hyp enthesis cells orginate from Sox9+ and Scx+ cells

Previous studies have demonstrated an expansion of fibrocartilage in the Achilles tendon entheses of P30 Hyp mice (Liang et al., 2009). To determine the time at which enthesopathy first develops, the presence of proteoglycans characteristic of chondrocyte matrix was evaluated by Safranin O staining of the Achilles tendon entheses of wild type (WT) and Hyp mice P7, P14, P30 and P60 (Fig. 1). The Achilles enthesis of P14 WT mice is characterized by sparse hypertrophic-appearing cells and a paucity of SafO+ matrix; by P30, both the SafO+ matrix and hypertrophic-appearing cells are absent. While the Hyp entheses are normal P7, with Safranin O staining matrix (SafO+) limited to the calcaneal secondary ossification center, hypertrophic-appearing cells and SafO+ matrix are present in the Achilles enthesis by P14, extending towards the tendon P30 and P60 (Fig. 1). This abnormal expansion of hypertrophic-appearing cells in Hyp entheses will be referred to as hypertrophic enthesopathy cells (HECs).

During embryonic development the enthesis develops from cells expressing the chondrogenic transcription factor Sox9 and Scx, a marker of tendon cells, with cells in the embryonic enthesis having been shown to express both Sox9 and Scx (Blitz et al., 2013; Sugimoto et al., 2013). Therefore, lineage tracing studies were performed to determine whether the cells in the WT post-natal enthesis and the HECs descend from Sox9+, Scx+, or Sox9+/Scx+ progenitors. Sox9-CreERT2: $R26R^{Tom}$, Scx-Cre:$R26R^{Tom}$, and Scx-CreERT: $R26R^{Tom}$ mice were generated in the Hyp background. Lineage tracing studies demonstrate that cells labeled with Scx-Cre populate the entheses of both WT and Hyp mice at P30 (Fig. 2A). The percent Scx-Tomato positive cells is not different between WT and Hyp entheses (WT vs Hyp: 75.1±1.9% vs 77.3±4.1%, $p>0.05$). Since the HECs in Hyp entheses appear by P14, induction of Scx-CreERT2 on P2 confirms that that P14 WT and Hyp enthesis cells are descendants of Scx-expressing cells (Fig. 2B). Because the HECs in Hyp entheses appear post-natally and Sox9 immunoreactive cells are present in the WT and Hyp entheses by P2 (Fig. 3A), Sox9-CreERT2 was induced by tamoxifen injection on P2, demonstrating that descendants of Sox9 expressing cells populate the entheses of both WT and Hyp mice as well (Fig. 3B). While few Sox9-CreERT2 labeled cells are observed in the proximal enthesis on P5, by P14, the entire enthesis and proximal portion of the tendon is populated with Sox9-CreERT2-labeled cells and by P30, descendants of these cells populate the entire enthesis and tendon in both WT and Hyp mice

(Fig. 3B). Thus, these results demonstrate that the HECs in Hyp mice originate from the same population of Scx and Sox9 expressing progenitors that give rise to the WT enthesis.

Hyp entheses are characterized by an expansion of Sox9+ cells

Since the cells in the enthesis of WT and Hyp mice descend from Sox9+ and Scx+ progenitors, we examined whether expression of chondrocyte markers persists in the pathologic HECs. Immunohistochemical analyses demonstrate the presence of Sox9 immunoreactive cells in the entheses of both WT and Hyp mice. However, by P30 there is an expansion in the domain of Sox9 expressing HECs in the Hyp entheses (Fig. 4A). In contrast, while cells expressing GFP under the Scx promoter (Scx-GFP) are present in the Achilles tendon entheses of WT and Hyp mice P14, by P30, no Scx-GFP expressing cells are seen in the proximal Achilles tendon enthesis in either WT or Hyp mice (Fig. 4B). Immunofluorescent staining for Sox9 confirms the presence of Sox9+/Scx+ cells in the enthesis of both WT and Hyp mice P14. However, Sox9 immunoreactivity in the proximal enthesis region persists P30 in Hyp, but not in WT mice (Fig. 4B). The expansion of Sox9 immunoreactive cells is evidenced by the significant increase in percent cells immunoreactive for Sox9 in P30 Hyp entheses (WT vs Hyp: 23.2±2.7% vs 52.1±1.6%, p value <0.05). Consistent with the time course of expansion of Safranin O and Sox9 positive cells in Hyp entheses, alkaline phosphatase activity is not altered in P5 Hyp entheses (data not shown), but is increased in Hyp entheses at P14 and P30 (Figure 5A). Like Sox9 expression, alkaline phosphatase staining is limited to the distal portion of WT entheses, and is expanded in the Hyp entheses. Immunohistochemistry for Proliferating Cell Nuclear Antigen (PCNA) demonstrates that the proliferation of enthesis cells decreases by P30, but the percentage of proliferating HECs is not different between WT and Hyp mice (Figure 5B, C). These results suggest that the mineralizing enthesopathy observed in XLH is due to persistence of Sox9 expressing, alkaline phosphatase positive chondrocytic cells in the enthesis.

BMP and IHH signaling is enhanced in Hyp entheses

Because the HECs have features characteristics of chondrocytes, including expression of Sox9 and presence of Safranin O stained matrix, signaling pathways that regulate chondrocyte differentiation were examined. BMP signaling induces phosphorylation of Smad 1/5/9 and expression of Sox9, promoting chondrocyte hypertrophy (Kobayashi et al., 2005; Kumar et al., 2012). Consistent with enhanced BMP signaling, an expansion of p-Smad 1/5/9 immunoreactive

cells is observed in P14 Hyp entheses and persists P30 (Fig. 6A). Although the percent immunoreactive p-Smad1/5/9 cells in WT and Hyp entheses is not different P7, an increase is seen in Hyp entheses compared to WT at P14 and P30 (WT vs Hyp, P7: 29.4±3.7% vs 29.3±4.5%,P14: 31.2±2.0% vs 57.4±6.6%, P30: 17.4±2.2% vs 44.5±0.5%, $p<0.05$ for P14 and P30). The BMP target gene IHH is necessary for both normal enthesis fibrocartilage development and chondrocyte maturation (Minina et al., 2001; Seki and Hata, 2004; Liu et al., 2013). Consistent with enhanced IHH signaling, an expansion of HECs expressing the IHH target and receptor, Patched, is observed in P14 Hyp entheses and persists P30 (Fig. 6B).

To confirm the enhanced BMP and IHH signaling in Hyp entheses, mRNA expression of BMP and IHH target genes was analyzed in P14 WT and Hyp entheses. These studies demonstrate increased expression of the BMP target gene *NOGGIN*, as well as that of *IHH* and its target genes *PTCH*, *RUNX2*, and *GLI1* (Fig. 6C). Expression of *ACAN* was also increased in the Hyp entheses. The mRNA expression of *PGR4*, a marker of articular cartilage, and *SCX*, a marker of tendon, was not different between the WT and Hyp entheses, confirming that the entheses analyzed were consistently isolated (Fig. 6C). BMP2 and BMP6 have been implicated in the development of enthesitis in a murine model of anklylosing spondylitis and BMP4 is necessary for the formation of the bony ridge onto which the deltoid tendon inserts (Lories et al., 2005; Blitz et al., 2009). Furthermore, enthesis cells are descendants of GDF5+ cells (Dyment et al., 2015). The mRNA expression of GDF5, but not that of BMP2, BMP4, or BMP6, was increased in Hyp entheses relative to WT, suggesting that increased expression of GDF5 underlies the enhanced BMP signaling in Hyp entheses (Fig. 6D) promoting aberrant chondrogenesis, leading to enthesopathy.

1.25D and FGF23Ab treatment of Hyp mice attenuates development of enthesopathy

To determine whether hypophosphatemia, impaired 1,25 dihydroxyvitamin D (1,25D) signaling, or enhanced FGF23 action contribute to the development of enthesopathy, Hyp mice were treated daily with 1,25D (175 ng/day) or three times per week with an FGF23 blocking antibody (FGF23Ab) starting on P2. Both treatments similarly increased serum phosphate levels and maintained normocalcemia (Table 1), consistent with previously reports (Liu et al., 2016). Safranin O staining demonstrates an attenuation of proteoglycans in the entheses of P30 Hyp mice treated with 1,25D or FGF23Ab (Fig. 7A, C). Both treatments decreased p-Smad 1/5/9,

Patched and Runx2 immunoreactivity in the Hyp entheses (Fig. 7A, C). These treatments also attenuated alkaline phosphatase activity (Fig. 7B, C).

1,25D suppresses BMP induced IHH signaling in chondrogenic cells

FGF23 impairs activation of vitamin D to 1,25D, thus both 1,25D and FGF23Ab treatment of Hyp mice increase 1,25D signaling (Liu et al., 2016). Since they also prevent the development of enthesopathy, it was hypothesized that 1,25D attenuates BMP induced IHH signaling. Since fibrocartilaginous enthesis cells have features of early chondrocytes, primary murine proliferative chondrocytes were treated with rhBMP2 with or without pretreatment with 1,25D. Treatment with rhBMP2 significantly induced the mRNA expression of *IHH* and its target genes compared to control (Fig. 8). 1,25D pretreatment attenuated BMP induction of *IHH* and blocked induction of *PTCH* and *GLI1* (Fig. 8*)*. These data implicate impaired 1,25D signaling in the pathogenisis of enthesopathy in XLH.

Discussion:

Our results demonstrate that post-natal enthesis maturation recapitulates the development of the embryonic tendon-bone insertion site (Blitz et al., 2013; Sugimoto et al., 2013). Post-natal Achilles tendon enthesis cells of both WT and Hyp mice originate from Scx and Sox9-expressing progenitors, with both Scx and Sox9 being expressed in this region post-natally. These studies also highlight the changing expression pattern of Scx, Sox9, and the IHH target gene PTCH in the normal post-natal maturing fibrocartilaginous enthesis. Expression of these markers in the WT enthesis is localized adjacent to the bone up to P14 and is focused more distally extending to the tendon as the enthesis matures by P30. Consistent with this, lineage tracing experiments revealed that while Gli1-CreERT2 labeled cells populate the proximal region of the WT murine enthesis early in post-natal life up to P13, by P56 the Gli1+ cells are limited to the distal region adjacent to the tendon (Schwartz et al., 2015).

The similar staining pattern of p-Smad1/5/9, Patched, and Sox9 in WT entheses at each age examined indicates that BMP signaling may stimulate IHH signaling in enthesis cells to promote and regulate fibrocartilage formation. In support of this, the current results and previous studies demonstrate that BMP signaling induces IHH signaling in chondrocytes (Grimsrud et al., 2001; Minina et al., 2001). BMP signaling is also necessary for the formation of the bony ridge onto which tendons insert (Blitz et al., 2009). Prior studies have shown that IHH signaling is

critical for the post-natal development of the enthesis, since ablation of the IHH target, Smoothened, from cells that express Scx disrupts the formation of fibrocartilage at the tendon-bone attachment site (Liu et al., 2013).

The current investigations characterize the time course of Hyp enthesopathy development post-natally, with Hyp entheses having increased expression of targets of BMP and IHH signaling P14 followed by an expansion of hypertrophic Safranin O and Sox9 positive cells in the proximal enthesis region by P30. These results, therefore, support the pathogenic role of BMP and IHH signaling in fibrocartilage development in XLH enthesopathy. Similar to Hyp enthesopathy, inflammatory enthesitis in mice and humans with ankylosing spondylitis is characterized by increased p-Smad1/5/9 immunoreactivity in affected entheses. (Lories et al., 2005). Like Hyp enthesopathy, this alternate model of enthesis pathology supports the importance of BMP signaling in the pathophysiology of mineralizing enthesopathy. Lineage tracing experiments demonstrated that fibrocartilage enthesis cells are descendants of GDF5+ precursors (Dyment et al., 2015) and the current investigations show that expression of GDF5 is increased in Hyp entheses, supporting a role for GDF5 in activating BMP signaling in Hyp entheses.

Our studies demonstrate that initiating 1,25D or FGF2Ab therapy prior to the development of enhanced BMP and IHH signaling in the Hyp entheses attenuates the development of enthesopathy. This contrasts with previous investigations demonstrating that treating of Hyp mice with 1,25D (3x/week) and oral phosphate supplementation starting week 3 and continuing to week 12 does not alter alkaline phosphatase staining in the Hyp entheses (Karaplis et al., 2012). This disparity suggests that once established, enthesopathy does not regress, or that phosphate supplementation antagonizes the beneficial effects of 1,25D. Regardless, our findings have important implications for the treatment of children with XLH, supporting the beneficial effects of early, consistent, and optimized 1,25D or FGF23Ab therapy to prevent the development of enthesopathies that cause pain and mobility issues in adults with XLH. A retrospective study failed to find a correlation between enthesopathy and proportion of life on phosphate and 1,25D therapy in XLH patients (Connor et al., 2015). It is possible that beneficial effects were not observed due to lack of optimization of 1,25D therapy (Liu et al., 2016), delay and/or inconsistent therapy, or the possibility that phosphate supplementation prevents the beneficial effects of 1,25D,

Several pathologic states with increased serum levels of FGF23, including transgenic mice over-expressing FGF23 (Karaplis et al., 2012), humans lacking DMP1 (Makitie et al., 2010), and mice and humans with XLH (Liang et al., 2009), exhibit enthesopathy, suggesting that enhanced FGF23 action plays a role in the pathogenesis of enthesopathy in XLH. However, based on our findings that treatment with 1,25D dramatically increased expression of FGF23 (Liu et al., 2016), yet prevented the enthesopathy in Hyp mice, it is unlikely that increased FGF23 action plays a major pathogenic role. Rather, the inhibition of BMP signaling seen in 1,25D treated chondrocytes, data showing that 1,25D inhibits BMP expression in vitro (Virdi et al., 1998; Fu et al., 2013), and the enhanced expression of IHH target genes in keratinocytes lacking the VDR (Lisse et al., 2014) all suggest that impaired 1,25D action underlies the enhanced BMP and IHH signaling in the entheses of Hyp mice. Thus, the current investigations implicate hypophosphatemia and/or decreased 1,25D action in the pathogenesis of enthesopathy in XLH.

Author Contributions: This work was supported by grants from the National Institutes of Health: K08 AR067854 (to ESL), R01 AR061376 and R01 AR 072650 (to MBD), and P30 AR061313. Authors' roles: Project design: E.S.L., M.B.D., Mouse colony management: E.S.L. Histological analyses: E.S.L., J.S.M. Molecular biology experiments: E.S.L., Cell culture: W.Z., E.S.L. Manuscript preparation: E.S.L., M.B.D.

References:

Akiyama, H., Kim, J. E., Nakashima, K., Balmes, G., Iwai, N., Deng, J. M., Zhang, Z., Martin, J. F., Behringer, R. R., Nakamura, T. et al. (2005). Osteo-chondroprogenitor cells are derived from Sox9 expressing precursors. *Proc Natl Acad Sci U S A* **102**, 14665-14670.

Bi, W., Deng, J. M., Zhang, Z., Behringer, R. R. and de Crombrugghe, B. (1999). Sox9 is required for cartilage formation. *Nature genetics* **22**, 85-89.

Blitz, E., Sharir, A., Akiyama, H. and Zelzer, E. (2013). Tendon-bone attachment unit is formed modularly by a distinct pool of Scx- and Sox9-positive progenitors. *Development* **140**, 2680-2690.

Blitz, E., Viukov, S., Sharir, A., Shwartz, Y., Galloway, J. L., Pryce, B. A., Johnson, R. L., Tabin, C. J., Schweitzer, R. and Zelzer, E. (2009). Bone ridge patterning during musculoskeletal assembly is mediated through SCX regulation of Bmp4 at the tendon-skeleton junction. *Developmental cell* **17**, 861-873.

Carpenter, T. O., Imel, E. A., Holm, I. A., Jan de Beur, S. M. and Insogna, K. L. (2011). A clinician's guide to X-linked hypophosphatemia. *Journal of bone and mineral research : the official journal of the American Society for Bone and Mineral Research* **26**, 1381-1388.

Chen, X., Macica, C. M., Dreyer, B. E., Hammond, V. E., Hens, J. R., Philbrick, W. M. and Broadus, A. E. (2006). Initial characterization of PTH-related protein gene-driven lacZ expression in the mouse. *Journal of bone and mineral research : the official journal of the American Society for Bone and Mineral Research* **21**, 113-123.

Connor, J., Olear, E. A., Insogna, K. L., Katz, L., Baker, S., Kaur, R., Simpson, C. A., Sterpka, J., Dubrow, R., Zhang, J. H. et al. (2015). Conventional Therapy in Adults With X-Linked Hypophosphatemia: Effects on Enthesopathy and Dental Disease. *The Journal of clinical endocrinology and metabolism* **100**, 3625-3632.

Dyment, N. A., Breidenbach, A. P., Schwartz, A. G., Russell, R. P., Aschbacher-Smith, L., Liu, H., Hagiwara, Y., Jiang, R., Thomopoulos, S., Butler, D. L. et al. (2015). Gdf5 progenitors give rise to fibrocartilage cells that mineralize via hedgehog signaling to form the zonal enthesis. *Developmental biology* **405**, 96-107.

Fu, B., Wang, H., Wang, J., Barouhas, I., Liu, W., Shuboy, A., Bushinsky, D. A., Zhou, D. and Favus, M. J. (2013). Epigenetic regulation of BMP2 by 1,25-dihydroxyvitamin D3 through DNA methylation and histone modification. *PloS one* **8**, e61423.

Genin, G. M., Kent, A., Birman, V., Wopenka, B., Pasteris, J. D., Marquez, P. J. and Thomopoulos, S. (2009). Functional grading of mineral and collagen in the attachment of tendon to bone. *Biophysical journal* **97**, 976-985.

Grimsrud, C. D., Romano, P. R., D'Souza, M., Puzas, J. E., Schwarz, E. M., Reynolds, P. R., Roiser, R. N. and O'Keefe, R. J. (2001). BMP signaling stimulates chondrocyte maturation and the expression of Indian hedgehog. *Journal of orthopaedic research : official publication of the Orthopaedic Research Society* **19**, 18-25.

Holm, I. A., Huang, X. and Kunkel, L. M. (1997). Mutational analysis of the PEX gene in patients with X-linked hypophosphatemic rickets. *American journal of human genetics* **60**, 790-797.

Howell, K., Chien, C., Bell, R., Laudier, D., Tufa, S. F., Keene, D. R., Andarawis-Puri, N. and Huang, A. H. (2017). Novel Model of Tendon Regeneration Reveals Distinct Cell Mechanisms Underlying Regenerative and Fibrotic Tendon Healing. *Scientific reports* **7**, 45238.

Jonsson, K. B., Zahradnik, R., Larsson, T., White, K. E., Sugimoto, T., Imanishi, Y., Yamamoto, T., Hampson, G., Koshiyama, H., Ljunggren, O. et al. (2003). Fibroblast growth factor 23 in oncogenic osteomalacia and X-linked hypophosphatemia. *The New England journal of medicine* **348**, 1656-1663.

Karaplis, A. C., Bai, X., Falet, J. P. and Macica, C. M. (2012). Mineralizing enthesopathy is a common feature of renal phosphate-wasting disorders attributed to FGF23 and is exacerbated by standard therapy in hyp mice. *Endocrinology* **153**, 5906-5917.

Killian, M. L. and Thomopoulos, S. (2016). Scleraxis is required for the development of a functional tendon enthesis. *FASEB journal : official publication of the Federation of American Societies for Experimental Biology* **30**, 301-311.

Kobayashi, T., Lyons, K. M., McMahon, A. P. and Kronenberg, H. M. (2005). BMP signaling stimulates cellular differentiation at multiple steps during cartilage development. *Proc Natl Acad Sci U S A* **102**, 18023-18027.

Kronenberg, H. M. (2003). Developmental regulation of the growth plate. *Nature* **423**, 332-336.

Kumar, M., Ray, P. and Chapman, S. C. (2012). Fibroblast growth factor and bone morphogenetic protein signaling are required for specifying prechondrogenic identity in neural crest-derived mesenchyme and initiating the chondrogenic program. *Developmental dynamics : an official publication of the American Association of Anatomists* **241**, 1091-1103.

Liang, G., Katz, L. D., Insogna, K. L., Carpenter, T. O. and Macica, C. M. (2009). Survey of the enthesopathy of X-linked hypophosphatemia and its characterization in Hyp mice. *Calcified tissue international* **85**, 235-246.

Lisse, T. S., Saini, V., Zhao, H., Luderer, H. F., Gori, F. and Demay, M. B. (2014). The vitamin D receptor is required for activation of cWnt and hedgehog signaling in keratinocytes. *Molecular endocrinology* **28**, 1698-1706.

Liu, C. F., Breidenbach, A., Aschbacher-Smith, L., Butler, D. and Wylie, C. (2013). A role for hedgehog signaling in the differentiation of the insertion site of the patellar tendon in the mouse. *PloS one* **8**, e65411.

Liu, C. F., Aschbacher-Smith, L., Barthelery, N. J., Dyment, N., Butler, D. and Wylie, C. (2012). Spatial and temporal expression of molecular markers and cell signals during normal development of the mouse patellar tendon. *Tissue engineering. Part A* **18**, 598-608.

Liu, E. S., Martins, J. S., Raimann, A., Chae, B. T., Brooks, D. J., Jorgetti, V., Bouxsein, M. L. and Demay, M. B. (2016). 1,25-Dihydroxyvitamin D Alone Improves Skeletal Growth, Microarchitecture and Strength in a Murine Model of XLH, Despite Enhanced FGF23 Expression. *Journal of bone and mineral research : the official journal of the American Society for Bone and Mineral Research*.

Liu, S., Zhou, J., Tang, W., Jiang, X., Rowe, D. W. and Quarles, L. D. (2006). Pathogenic role of Fgf23 in Hyp mice. *American journal of physiology. Endocrinology and metabolism* **291**, E38-49.

Lories, R. J., Derese, I. and Luyten, F. P. (2005). Modulation of bone morphogenetic protein signaling inhibits the onset and progression of ankylosing enthesitis. *J Clin Invest* **115**, 1571-1579.

Makitie, O., Pereira, R. C., Kaitila, I., Turan, S., Bastepe, M., Laine, T., Kroger, H., Cole, W. G. and Juppner, H. (2010). Long-term clinical outcome and carrier phenotype in autosomal recessive hypophosphatemia caused by a novel DMP1 mutation. *Journal of bone and mineral research : the official journal of the American Society for Bone and Mineral Research* **25**, 2165-2174.

Miedlich, S. U., Zalutskaya, A., Zhu, E. D. and Demay, M. B. (2010). Phosphate-induced apoptosis of hypertrophic chondrocytes is associated with a decrease in mitochondrial membrane potential and is dependent upon ERK1/2 phosphorylation. *J Biol Chem* **285**, 18270-18275.

Minina, E., Wenzel, H. M., Kreschel, C., Karp, S., Gaffield, W., McMahon, A. P. and Vortkamp, A. (2001). BMP and Ihh/PTHrP signaling interact to coordinate chondrocyte proliferation and differentiation. *Development* **128**, 4523-4534.

Murchison, N. D., Price, B. A., Conner, D. A., Keene, D. R., Olson, E. N., Tabin, C. J. and Schweitzer, R. (2007). Regulation of tendon differentiation by scleraxis distinguishes force-transmitting tendons from muscle-anchoring tendons. *Development* **134**, 2697-2708.

Pryce, B. A., Brent, A. E., Murchison, N. D., Tabin, C. J. and Schweitzer, R. (2007). Generation of transgenic tendon reporters, ScxGFP and ScxAP, using regulatory elements of the scleraxis gene. *Developmental dynamics : an official publication of the American Association of Anatomists* **236**, 1677-1682.

Sabbagh, Y., Carpenter, T. O. and Demay, M. (2005). Hypophosphatemia leads to rickets by impairing caspase-mediated apoptosis of hypertrophic chondrocytes. *Proc Natl Acad Sci* **102**, 9637-9642.

Schwartz, A. G., Long, F. and Thomopoulos, S. (2015). Enthesis fibrocartilage cells originate from a population of Hedgehog-responsive cells modulated by the loading environment. *Development* **142**, 196-206.

Schwartz, A. G., Pasteris, J. D., Genin, G. M., Daulton, T. L. and Thomopoulos, S. (2012). Mineral distributions at the developing tendon enthesis. *PloS one* **7**, e48630.

Schweitzer, R., Chyung, J. H., Murtaugh, L. C., Brent, A. E., Rosen, V., Olson, E. N., Lassar, A. and Tabin, C. J. (2001). Analysis of the tendon cell fate using Scleraxis, a specific marker for tendons and ligaments. *Development* **128**, 3855-3866.

Seki, K. and Hata, A. (2004). Indian hedgehog gene is a target of the bone morphogenetic protein signaling pathway. *J Biol Chem* **279**, 18544-18549.

Soeda, T., Deng, J. M., de Crombrugghe, B., Behringer, R. R., Nakamura, T. and Akiyama, H. (2010). Sox9-expressing precursors are the cellular origin of the cruciate ligament of the knee joint and the limb tendons. *Genesis* **48**, 635-644.

St-Jacques, B., Hammerschmidt, M. and McMahon, A. P. (1999). Indian hedgehog signaling regulates proliferation and differentiation of chondrocytes and is essential for bone formation. *Genes & development* **13**, 2072-2086.

Sugimoto, Y., Takimoto, A., Akiyama, H., Kist, R., Scherer, G., Nakamura, T., Hiraki, Y. and Shukunami, C. (2013). Scx+/Sox9+ progenitors contribute to the establishment of the junction between cartilage and tendon/ligament. *Development* **140**, 2280-2288.

Sugita, D., Yayama, T., Uchida, K., Kokubo, Y., Nakajima, H., Yamagishi, A., Takeura, N. and Baba, H. (2013). Indian hedgehog signaling promotes chondrocyte differentiation in enchondral ossification in human cervical ossification of the posterior longitudinal ligament. *Spine* **38**, E1388-1396.

Thomopoulos, S., Genin, G. M. and Galatz, L. M. (2010). The development and morphogenesis of the tendon-to-bone insertion - what development can teach us about healing. *Journal of musculoskeletal & neuronal interactions* **10**, 35-45.

Virdi, A. S., Cook, L. J., Oreffo, R. O. and Triffitt, J. T. (1998). Modulation of bone morphogenetic protein-2 and bone morphogenetic protein-4 gene expression in osteoblastic cell lines. *Cellular and molecular biology* **44**, 1237-1246.

Zelzer, E., Blitz, E., Killian, M. L. and Thomopoulos, S. (2014). Tendon-to-bone attachment: from development to maturity. *Birth defects research. Part C, Embryo today : reviews* **102**, 101-112.

Figures

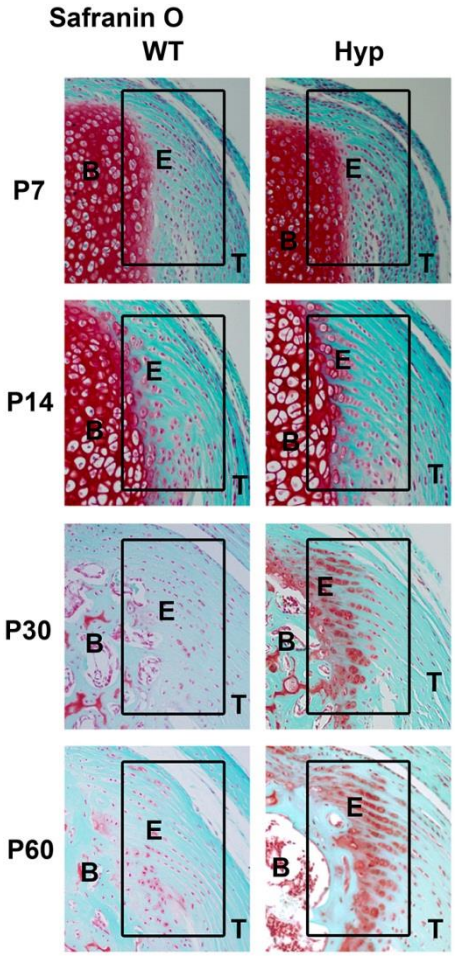

Figure 1. **Hyp entheses exhibit an expansion of Safranin O+ cells**: Safranin O staining of WT and Hyp entheses. Enthesis region is outlined with a black box (B – bone, E – enthesis, T-tendon). Data are representative of 3 mice per age/genotype group.

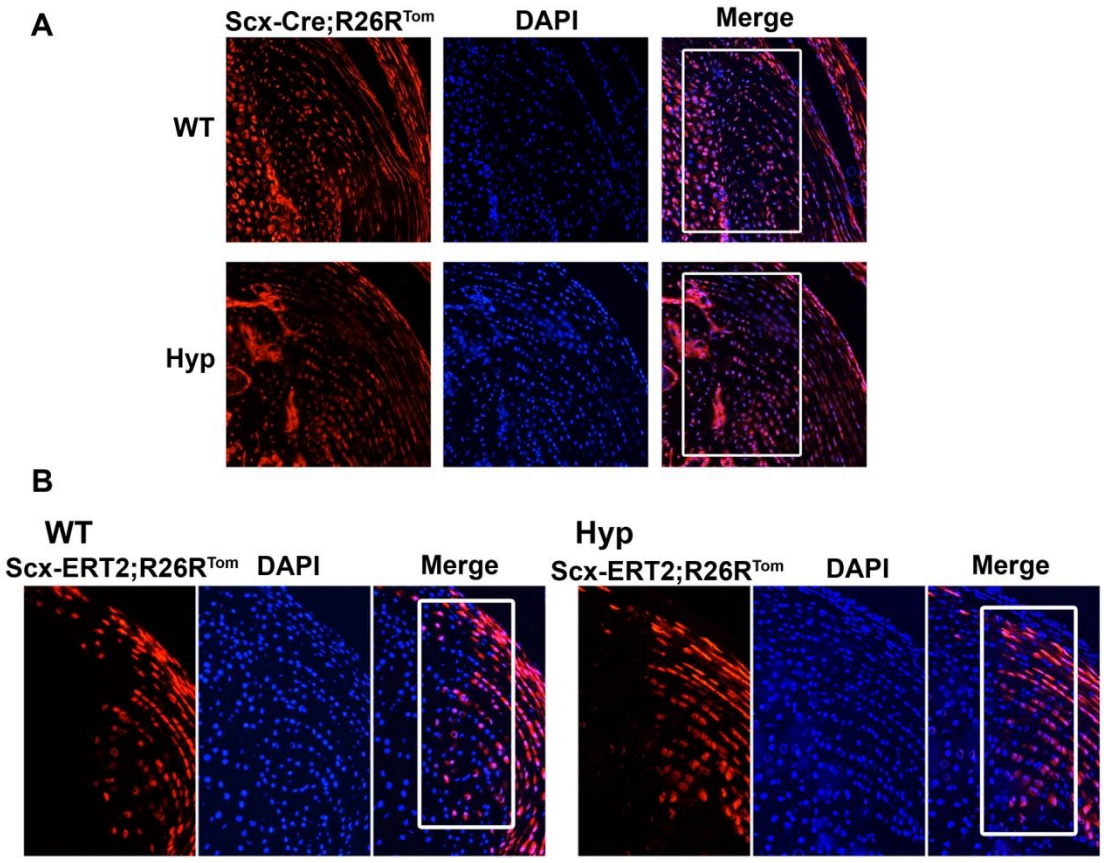

Figure 2. **Hyp enthesopathy cells descend from Scx+ progenitors**: A. Representative images of P30 entheses from Scx-Cre;R26R^{Tom} WT and Scx-Cre;R26R^{Tom} Hyp mice. Data are representative of 3 mice per age/genotype group. B. Representative images of entheses from Scx-CreERT2;R26R^{Tom} WT and Scx-CreERT2;R26R^{Tom} Hyp mice. A single dose of tamoxifen was injected P2 and mice were sacrificed P14. Data are representative of at least 2 mice per age/genotype group.

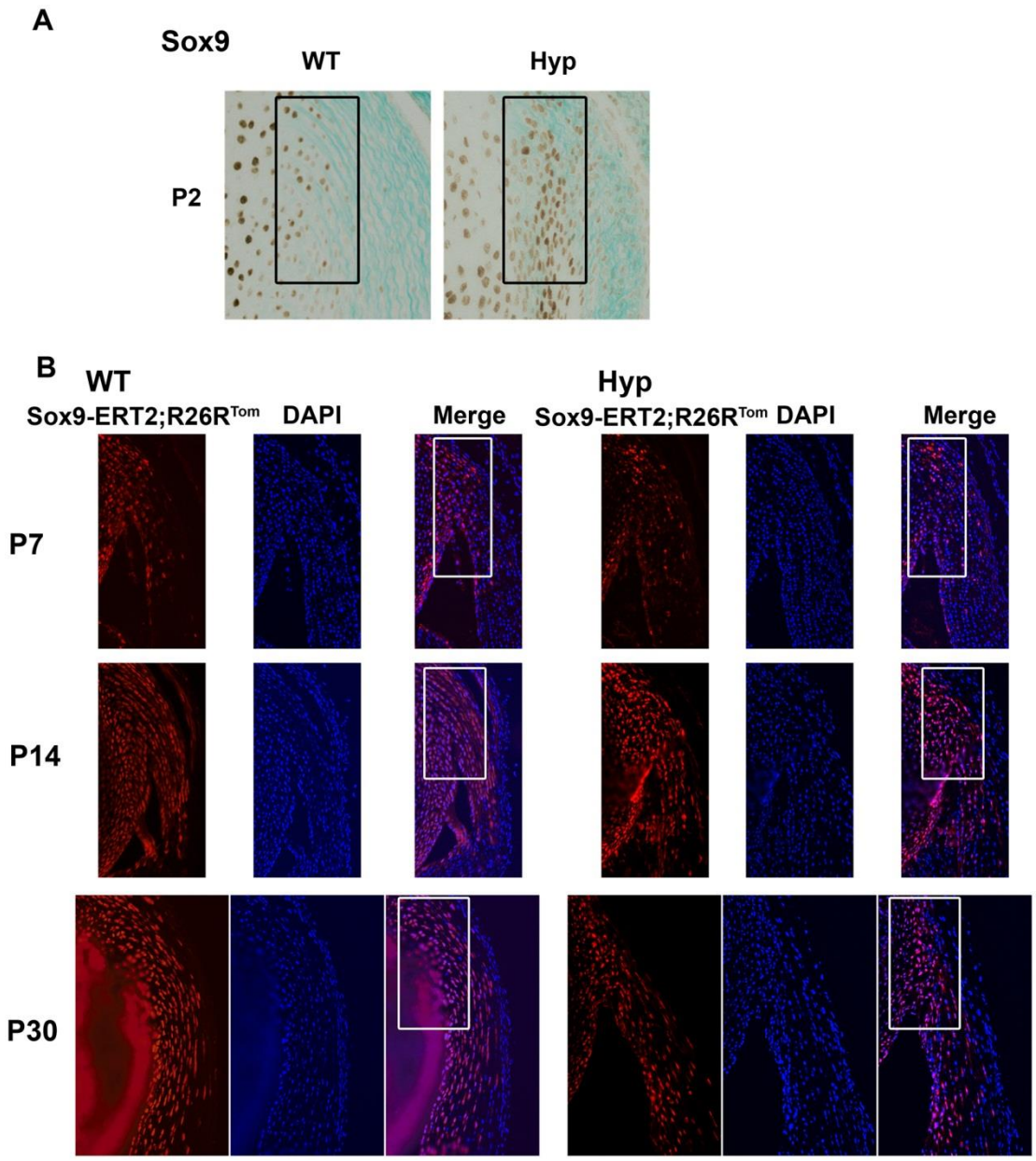

Figure 3. Hyp enthesopathy cells descend from Sox9-expressing cells: A. Immunohistochemistry for Sox9 in P2 WT and Hyp entheses. B. Representative images of entheses from Sox9-CreERT2;R26R^{Tom} WT and Sox9-CreERT2;R26R^{Tom} Hyp mice. A single dose of tamoxifen was injected P2 and mice were sacrificed P5, P14, and P30. Data are representative of 3 mice per age/genotype group.

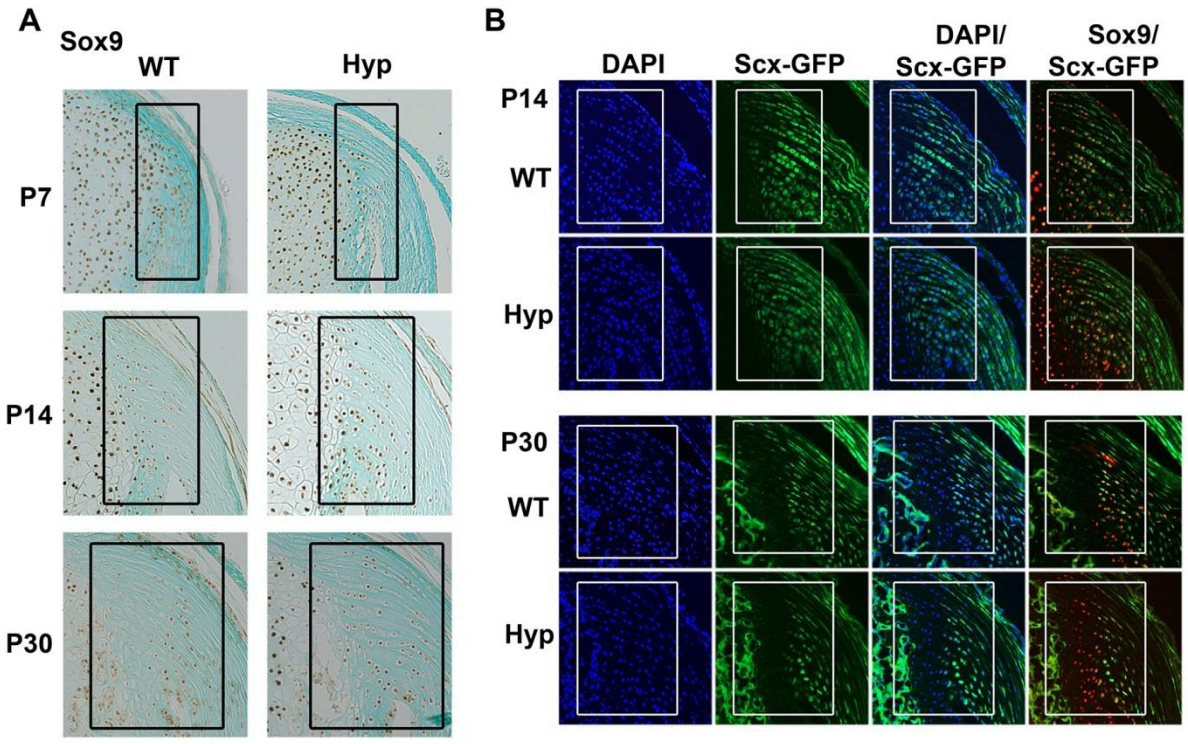

Figure 4. **Proximal enthesis cells in P30 Hyp mice exhibit persistent and enhanced Sox9 expression** : A. Immunohistochemistry for Sox9 in WT and Hyp entheses. B. Entheses from P14 and P30 WT and Hyp mice expressing scleraxis-GFP (Scx-GFP) (green). Sox9 immunofluorescence staining (red) in the entheses of Scx-GFP WT and Hyp mice. Enthesis region is outlined with a black or white box. Data are representative of 3 mice per genotype/treatment group.

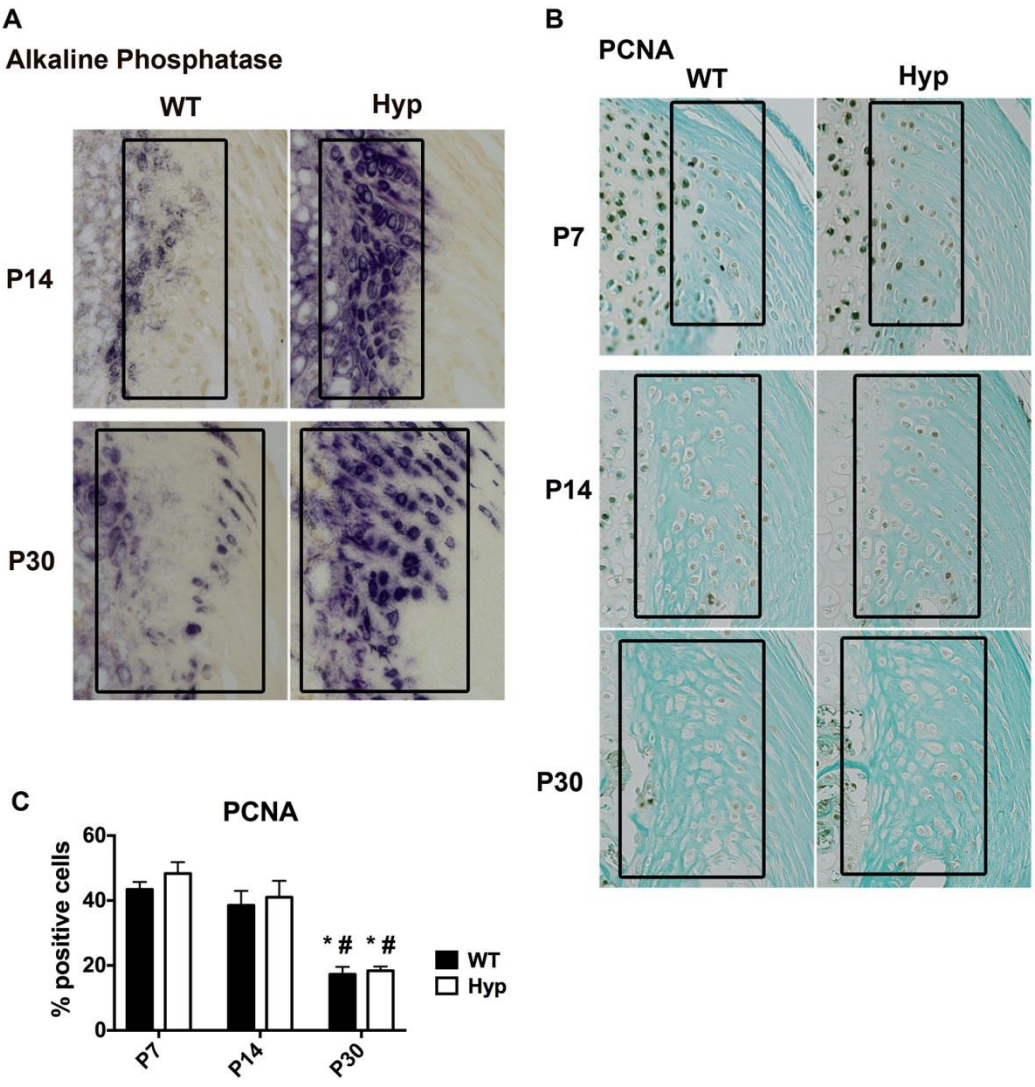

Figure 5: Hyp entheses have increased alkaline phosphatase activity but do not have increased proliferation. A. Alkaline phosphatase stain on entheses from P14 and P30 WT and Hyp entheses. B. Immunohistochemistry for PCNA in WT and Hyp entheses. Enthesis region is outlined with a black box. C. Quantitation of percent PCNA positive cells in WT and Hyp entheses. Data are representative of 3 mice per genotype group. * =p value <0.05 vs P7, # = p value <0.05 vs P14

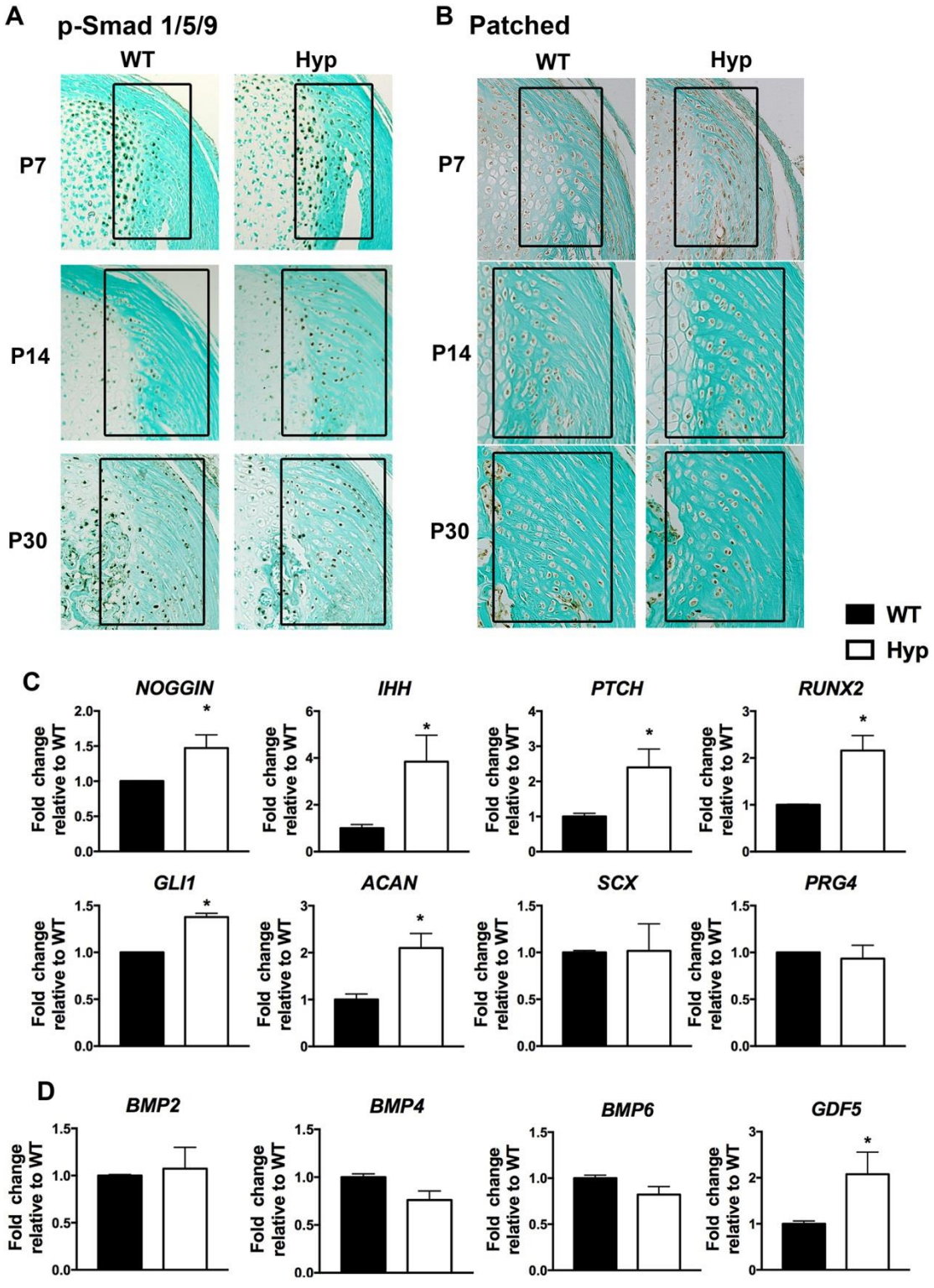

Figure 6. **Hyp entheses exhibit increased expression of BMP and IHH signaling target genes**: Immunohistochemistry for p-Smad1/5/9 (A) and Patched (PTCH) (B) in WT and Hyp entheses. Enthesis region is outlined with a black box. Data are representative of 3 mice per age/genotype group. C. mRNA expression of BMP and IHH signaling target genes, *ACAN*, *PGF4*, and *SCX* in P14 WT and Hyp entheses. Gene expression is normalized to that of WT. D. mRNA expression of *BMPs* and *GDF5* in P14 WT and Hyp entheses. Gene expression is normalized to that of WT. Data are representative of 3 mice per age/genotype group * =p value <0.05 vs WT

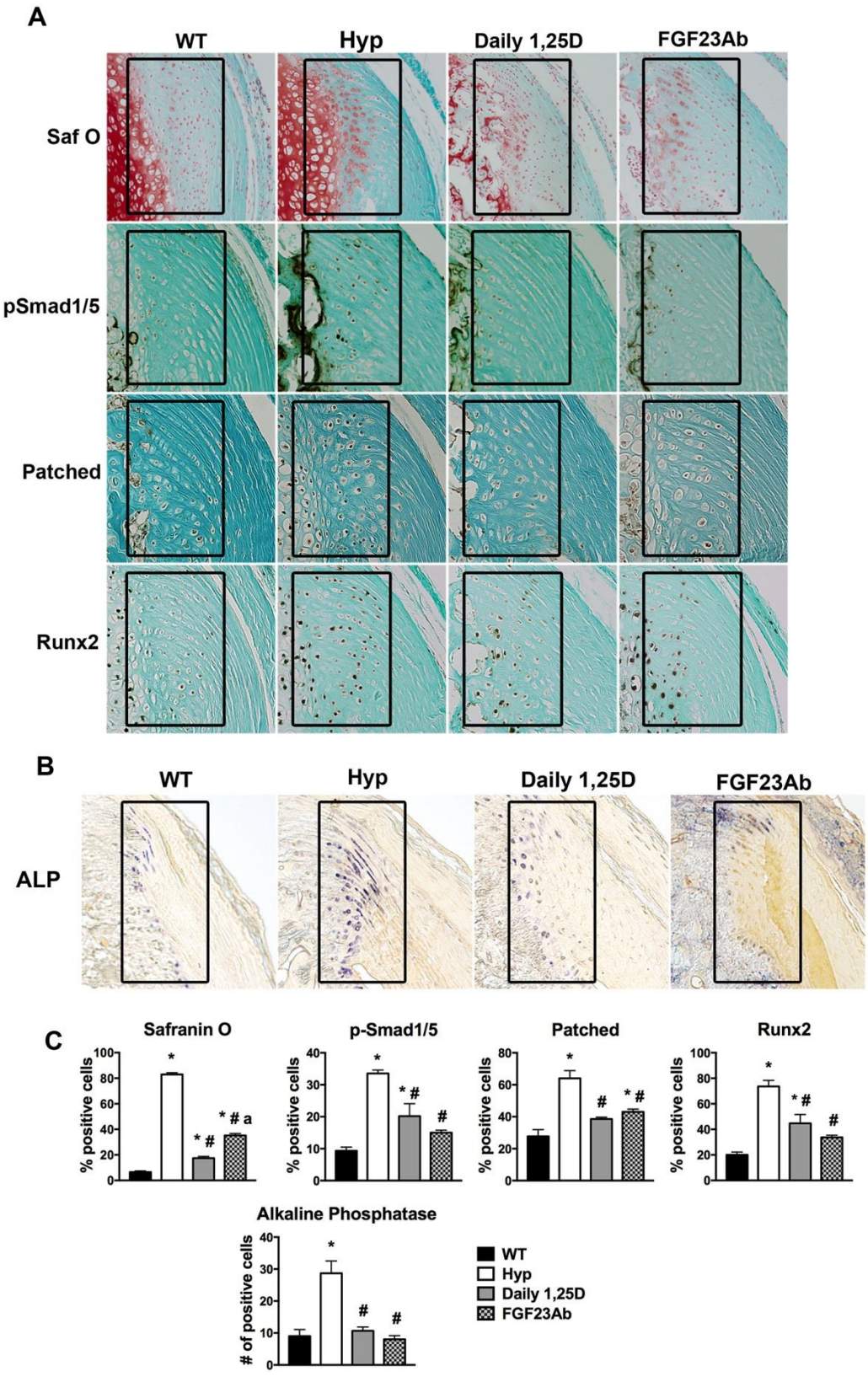

Figure 7. **Treatment of Hyp mice with 1,25D or FGF23Ab attenuates enthesopathy**: A. Safranin O staining and p-Smad1/5/9, PTCH, and Runx2 immunohistochemistry was performed on entheses from P30 WT and Hyp control mice and Hyp mice treated with 1,25D or FGF23Ab. B. Alkaline phosphatase stain on entheses from P75 WT and Hyp control mice and Hyp mice treated with 1,25D or FGF23Ab. Enthesis region is outlined with a black box. Data are representative of 3 mice per genotype/treatment group. C. Quantitation of percent Safranin O positive, percent cells immunoreactive for p-Smad1/5/9, PTCH, and Runx2, and number of alkaline phosphatase positive cells. *= p value < 0.05 vs WT, # = p value <0.05 vs Hyp, a = p value <0.05 vs 1.25D

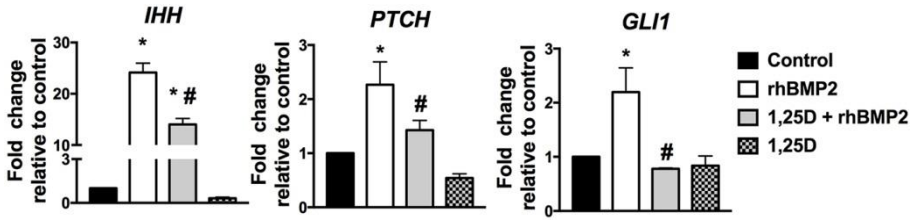

Figure 8. 1,25D treatment of chondrogenic cells inhibits BMP induced IHH signaling: Primary murine chondrocytes treated with 150 ng/mL of rhBMP2 with or without pretreatment with 10^{-8}M 1,25D. Gene expression analysis performed for *IHH*, *PTCH*, and *GLI1*. Data are representative of that obtained from 3 experiments. *= p value < 0.05 vs control, #= p value <0.05 vs hrBMP2.

Table 1:

	WT	Hyp	Daily 1,25D	FGF23Ab
Ca (mg/dL)	10.2±0.7	9.6±0.1	10.3±0.2	9.4±0.2
Pi (mg/dL)	11.0±0.6	5.9±0.4*	7.9±0.3*#	6.5±0.2*#a

Table 1. Serum parameters in Hyp mice treated with daily 1,25D or FGF23Ab. Data represent the mean and SEM of that obtained from 3 mice per genotype/treatment group. Ca = serum calcium, Pi = serum phosphorus * =p value <0.05 vs WT, # =p value <0.05 vs Hyp Con, a =p value <0.05 vs Daily 1,25D.